

On recording sea surface elevation with accelerometer buoys: lessons from ITOP (2010)

Clarence O. Collins III · Björn Lund · Takuji Waseda · Hans C. Graber

Received: 22 January 2014 / Accepted: 28 April 2014 / Published online: 29 May 2014
© Springer-Verlag Berlin Heidelberg 2014

Abstract Measurements of significant wave height are made routinely throughout the world's oceans, but a record of the sea surface elevation (η) is rarely kept. This is mostly due to memory limitations on data, but also, it is thought that buoy measurements of sea surface elevation are not as accurate as wave gauges mounted on stationary platforms. Accurate records of η which contain rogue waves (defined here as an individual wave at least twice the significant wave height) are of great interest to scientists and engineers. Using field data, procedures for tilt correcting and double integrating accelerometer data to produce a consistent record of η are given in this study. The data in this study are from experimental buoys deployed in the recent *Impact of Typhoons on the Ocean in the Pacific* (ITOP) field experiment which occurred in 2010. The statistics from the ITOP buoys is under that predicted by Rayleigh theory, but matches the distributions of Boccotti and others (Tayfun and Fedele) (Ocean Eng 34:1631-1649, 2007). Rogue waves were recorded throughout the experiment under various sea state conditions. Recommendations, as a result of lessons learned during ITOP, are made for the routine recording of η which may not add significantly to the existing data burden. The hope is that we might one day collect a worldwide database of rogue waves from the existing

buoy network, which would progress our understanding of the rogue wave phenomenon and make work at sea safer.

Keywords Ocean waves · Rogue waves · Buoy measurements · In situ data · ITOP · Wave statistics · Extreme waves · Wind waves · Sea surface elevation

1 Introduction

Waves on the open ocean are commonly represented as a stochastic process. Waves on a record of sea surface elevation (η) do not retain individuality because they are the superposition of many waves with random phase. Therefore, a convention has been established in which consecutive crossings of the mean water level qualify as an apparent wave. Significant wave height, H_s , is a metric which characterizes the average height of waves within a single record, and typical record lengths run from 15 min to 1 h. The maximum wave height (H_{\max}) divided by the average wave height is an abnormality index (AI). Rogue¹ waves are defined through meeting sufficiently high AI criteria, which amounts to choosing a wave height suitably far out on the tail of an exceedance distribution function (EDF). The criteria are commonly set as $H_{\max}/H_s > 2$, which occurs for one out of 3,000 waves assuming Gaussian (linear) wave theory (Waseda et al. 2009). Rogue waves are important for design of platforms and for safety at sea. Understanding rogue waves, in particular their generating mechanism and their connection with accidents at sea, has been a very active part of ocean research in recent years (Cavaleri

Responsible Editor: Val Swail

This article is part of the Topical Collection on the *13th International Workshop on Wave Hindcasting and Forecasting in Banff, Alberta, Canada October 27 - November 1, 2013*

C. O. Collins III (✉) · B. Lund · H. C. Graber
University of Miami, 4600 Rickenbacker Causeway,
Miami, FL 33149, USA
e-mail: Tripphysicist@gmail.com

T. Waseda
Graduate School of Frontier Sciences, University of Tokyo,
5-1-5 Kashiwanoha, Kashiwa City, Chiba 277-8563, Japan

¹ Also referred to as an extreme wave, freak wave, killer wave, three sisters, wall of water, hole in the sea, abnormal wave, etc. Some confusion has come over nomenclature. To clarify, here, we only mean to represent a wave far out on the probability tail and do not necessarily imply connection to a generation mechanism or to any special dynamic property.

et al. 2012; Dysthe et al. 2008; Guedes Soares et al. 2004; Onorato et al. 2009; Tamura et al. 2009; Waseda et al. 2009; Waseda et al. 2012). Good quality field data, even though very valuable, have been difficult to come by: field data have simply been difficult to obtain (this is especially true for directional wave data (Waseda et al. 2011)), there are instrumental uncertainties which amount to errors in the measurement of sea surface elevation (Forristall et al. 2002), and parameters such as H_{\max} are not routinely reported. Platform-mounted systems (e.g., laser altimeters) are probably best suited to make accurate recordings of η , but these systems are often operated by private companies on platforms located in marginal seas. It would be useful and convenient to be able to obtain routine estimates of H_{\max} from our existing public network of deep sea buoys, most of which are accelerometer buoys.

Following up on an introduction to a high-quality dataset from a recent Office of Naval Research (ONR) field experiment (Collins III et al. 2014), we aim to delve into specific technical difficulties in retrieving η , and therefore H_{\max} , from accelerometer buoys. Additionally, we will make recommendations for best practices which could be implemented in the existing worldwide buoy network. The organization is as follows: section 1.1 closes the introduction with a review of platforms used for measurement of η . Section 2 introduces the ONR field experiment and details the measurement platform featured in this study. Section 3 delves into problems encountered during data analysis and solutions to these problems. Section 4 is a discussion of some of the results and suggestions for routine measurement η .

1.1 Review field platforms for study of rogue waves

Much of this section follows from the very thorough review of measurements in (Dysthe et al. 2008), but here, the focus is on the measurement platforms and on the expected performance. For more information please refer to their study. Many platforms report the time series of sea surface elevation, η . Agreement on η , in contrast to measurements of bulk parameters (but much like the measurement of the full 1-D spectrum), is not usually consistent. Measurement platforms operate on different physical principles, in different reference frames (i.e., fully or partially Eulerian or Lagrangian), and most require a transfer function to translate the quantity which is actually measured to η (e.g., Young (1994) appendix 1) and perhaps additional transfer functions to correct for inaccurate frequency responses (Steele et al. 1985). So, it is of no surprise when differences are observed in the recordings of η even in collocated systems (Forristall et al. 2002). On top of this, there are many different companies which produce these platforms, so even platforms that are similar in most ways manufactured by competing companies may give different answers because of idiosyncrasies. There are also issues with processing data (or not processing as the case may be), which may influence the final output of

η . When sensors disagree, often we do not have a way to tell which is more accurate. Perhaps Forristall (2000) put it best, “Measurements from one type of sensor often disagree with those from another type, and there is no agreement on which is correct. The basic problem is the lack of any absolute standard against which the accuracy of the sensors can be judged.”

General classes of instruments which report η include altimeters (laser, radio, acoustic, etc.), radar, wave staffs (capacitance, resistance, inductance, etc.), buoys (accelerometer, displacement, GPS, etc.), and subsurface pressure sensors. Pure Eulerian measurements from instruments mounted on stationary platforms such as altimeters and wave staffs have historically been favored. Indeed, in an assessment of a wave staff, a laser altimeter, two radars, and two step gauge systems, Forristall et al. (2002) showed that the most consistent measurements were made by the wave staff and laser systems. On the other hand, platform instruments are more or less susceptible to contamination by bubbles, foam, and sea spray (Magnusson and Donelan 2013) with the radars being particularly susceptible. Unfortunately, even though several buoys were present, buoy measurements were not included in the Forristall et al. (2002) comparison. Previous studies have shown that buoy data typically give statistics under that of Gaussian wave theory. This may be a result of broad-band and/or nonlinear seas, in which the Rayleigh distribution is no longer appropriate. It has been proposed that this may be due to buoys’ free horizontal movement which may allow for avoiding the highest waves (Krogstad and Barstow 2000). Also, Dysthe et al. (2008) state that there is a belief that the wave profiles recorded by buoys are “less accurate,” but this statement was not substantiated. Forristall (2000) cites the semi-Lagrangian nature of surface-following buoys and influence of the mooring line as possible drawbacks. The motion of purely Lagrangian wave measurements will cancel out the second-order nonlinearities in wave crests (Forristall 2000; Srokosz and Longuet-Higgins 1986). While there may be shortcomings, buoys have the potential for obtaining autonomous measurements of η in the deep sea, so a better understanding of these measurements is a worthwhile endeavor.

Although the focus of this study is the proper processing of accelerometer buoys, some basic, intuitive recommendations can be made here which may be applied, in general, to measurements of η for rogue wave studies:

- Measurements should not be made where other environmental factors strongly affect the wave shape (e.g., in strong current gradients, reflections from platforms, sharply varying and/or shallow bathymetry)
- It is preferable that sensors measure η directly
- If a transfer function is necessary, results from sensors which invoke a small amplitude assumption (e.g., pressure sensors) may be invalid particularly in the cases of interest (i.e., waves with extreme heights and steepness)

- It is necessary to develop quality control measures which will aid in understanding the strengths and weaknesses of the data

2 Experimental setup

2.1 ITOP experiment

In late 2010, the air-sea interaction research group at the University of Miami (UM) was involved in the international, collaborative, ONR-sponsored field campaign called Impact of Typhoons on the Ocean in the Pacific (ITOP) (D'Asaro et al. 2013) 750 km off the eastern coast of Taiwan in the Philippine Sea. The UM group installed two moorings, and each mooring site included two buoys. One buoy with a 6-m naval oceanographic meteorological automatic device (NOMAD)-type hull dubbed the extreme air-sea interaction (EASI) buoy (Drennan et al. 2014; Collins III et al. 2014) was moored to the sea bed. The second buoy, an air-sea interaction spar (ASIS) buoy (Graber et al. 2000), was tethered to EASI by a 60-m braided steel line.

Each EASI buoy (Fig. 1), to be described further in section 2.2, was moored to the sea floor in a depth of ~5,500 m. A single point inverse catenary-style mooring system was employed with a scope (i.e., ratio of mooring length to water depth) of 1.26 to allow the buoy to follow the surface relatively unobstructed. The attachment point was a stainless steel yoke, the purpose of which was to try and further isolate the buoy from mooring forces. The ~3,100-kg mooring anchors (locomotive wheels) were located at 127.25° E, 19.63° N and 126.96° E, 21.23° N which amounts to a separation of about 180 km. These are referred to as the northern (-N) and southern (-S) moorings, respectively.



Fig. 1 EASI buoy off the stern of the R/V Roger Revelle after deployment during the 2010 ITOP experiment

Further details of the mooring components may be found in Drennan et al. (2014). On September 17th, (year day (YD) 260), during Typhoon Fanapi, the tether sheared apart and ASIS-N had to be recovered early. Similarly, on October 22nd (YD 295), during Typhoon Megi, the ASIS-S broke free of its tether requiring recovery. The EASI buoys operated continuously for approximately 4 months, also described in full by Drennan et al. (2014), endured the relatively close passages of four major tropical cyclones (TC) and received significant swell which radiated from a fifth TC. This dataset includes directional and non-directional wave information (Collins III et al. 2014).

2.2 Buoy design

EASI's ship-like hull is based on a NOMAD design which originated in the 1940s as part of the U.S. Navy's offshore data collection program and has subsequently seen modern deployment by the National Oceanic and Atmospheric Administration's (NOAA) National Data Buoy Center (NDBC) and the Canadian Marine Environmental Data Service (MEDS). The configuration used in ITOP is completely unique from previous NOMAD deployments. Of interest to this study is the use of a motion pack which measured all 6 degrees of freedom (i.e., heave, pitch roll, surge, sway, yaw) which consisted of a triaxial linear accelerometer (Columbia Research Laboratories SA307-HPTX), three orthogonally mounted rate gyros (Systron Donner model QRS110050 or SDG1000), and a compass (Precision Navigation TCM-2). Collins et al. (2014) showed that the EASI buoys could be treated as heave-pitch-roll surface-following systems in order to obtain directional wave spectra. Crucially, Drennan et al. (2014) showed that, for the energy containing region of the sea surface elevation spectrum, the EASI platform is a near perfect surface follower. For bulk parameters including H_s , EASI platforms were extensively compared and validated in Collins et al. (2014).

Lastly, the physical size of the buoy (6 m × 3 m × 3 m) acts as a low-pass filter. The buoy response falls off at wavelengths corresponding to ~0.45 Hz and shorter. Due to this size filtering, the statistics of short, small seas will not be accurately represented. This should not present a problem because the mean and standard deviation peak frequency over the experiment was 0.125 ± 0.024 Hz (corresponding peak wavelength of 124 ± 50 m). So, spectral parameters remain generally unaffected by the size filtering, particularly so for the highest sea states.

3 Data processing

3.1 Double integration

The nearly continuous dataset was split up into 30-min blocks (5,990 and 5,101 blocks for EASI-N and EASI-S,

respectively). For each block, signals were recorded at 20 Hz, and average parameters and spectra were calculated from these signals. Calculating surface elevation from the accelerometer requires double integration of the tilt-corrected acceleration signal (A_z). Integration was performed in frequency space by applying a fast Fourier transform (FFT) and then multiplying by a transfer function as follows:

$$\iint x(t)dt = \int_{-\infty}^{\infty} \frac{1}{(2\pi if)^2} \hat{x}(f)df$$

A high-pass filter (rectangular) was applied to deal with low-frequency noise before returning the signal to a time series via inverse FFT. The convolution of this high-pass filter introduced some spectral leakage. It is believed that this spectral leakage is the root of artificial amplitude enhancement at the margins of some low sea state records.

In the EASI-S, these marginal errors were exacerbated by 60–90-s flatline in all recorded channels at the beginning of every one-fourth block. As a result of this artifact, many more waves qualified as rogue in the EASI-S dataset during the preliminary analysis. Because many of these waves were located in the margins, these waves were identified as a spurious artifact of the processing. Perhaps the simplest fix was chosen: the first 90 s of A_z was removed from every 30-min block in EASI-S. The loss of waves from good parts of the record (and those records without errors) was accepted for the tradeoff of reducing this error and maintaining simple analysis procedures. Figure 2 shows a comparison of the surface elevation, η , from the original A_z and one with the first 90 s removed. It can be seen that the effect is localized to the first (not shown) and last few wavelengths (Fig. 2) along the margins. The plot also shows the Blackman-Harris (BH) window which was used before applying a FFT for spectral analysis. The BH window removes the artificial part of the

record; therefore, these errors were not factored into the original calculation of spectral parameters (i.e., H_s).

Errors in the margins of surface elevation records have previously been documented. Using a wavelet transform to integrate acceleration data, Chuang et al. (2009) and Doong and Wu (2010) found similar marginal errors. They concluded, though did not convincingly document, that the problem was a combined effect of discretizing a continuous wavelet transform and biased energy in the marginal area of the scalogram. The impetus for their integration by wavelet method was that rogue waves are inherently a non-stationary process, for which the use of the Fourier transform becomes a questionable practice. Stationarity may also be an issue here, but it is suspected that a better filter (e.g., fourth-order Butterworth) may well alleviate this error. However, this is left to be confirmed in the future.

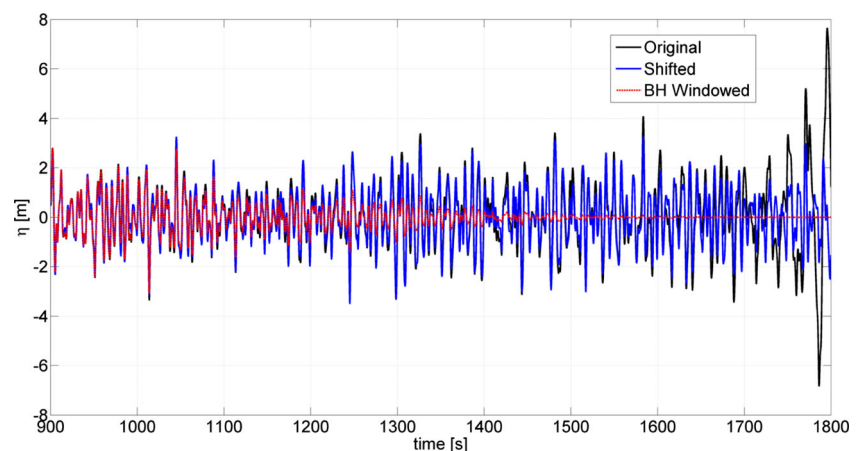
3.2 Tilt correction

Before doubly integrating, the accelerometer must be tilt corrected to give true vertical acceleration, A_z :

$$\eta = \iint A_z dt dt = \iint (-a_1 \sin\theta + a_2 \cos\theta \sin\varphi + a_3 \cos\theta \cos\varphi - g) dt dt \quad (1)$$

where a_1 , a_2 , a_3 , θ , φ , and g are surge, sway, heave, pitch, roll, and the gravitation constant, respectively. Bender et al. (2010) reported several methods of calculating the vertical acceleration on a 3-m discus buoy during Hurricane Katrina in the Gulf of Mexico. Without tilt correction, as given by Anctil et al. (1994), of the “strapped down” vertical accelerometer, they reported an average error of 26 % and up to 56 % error in H_{m0} during the peak of Hurricane Katrina. This is due to *sustained* heel (i.e., tipping) of the buoy. Instantaneous tilt (i.e., pitch and roll), as long as it is zero averaged over the record, should have little apparent effect on H_{m0} . Instantaneous tilt also has little effect on recorded shape of small

Fig. 2 The second half of a 30-min analysis block from EASI-S. The *solid black line* shows the surface elevation as a result of integrating the flatlined A_z signal. The corrected data (beginning the analysis after the flatline, referred to as shifted) are shown in *solid blue*. The *red dashed line* shows the signal after the application of a Blackman-Harris window as part of the spectral analysis



amplitude surface waves. This is intuitive in terms of small angles of pitch and roll. Under circumstances where pitch and roll are more substantial (i.e., $> \sim 15^\circ$), instantaneous tilt does have a major impact on shape and size of waves. This is particularly the case for extreme waves in a record because they are often accompanied by large buoy pitch and roll.

From Eq. 1, heave, pitch, roll, surge, and sway are the constituent inputs for calculating A_z . The top panel of Fig. 3 shows a 30-s time series of the A_z , heave, surge, and sway. The middle panel shows the same 30 s of pitch, and roll signals. Pitch and roll never breach $\pm 10^\circ$. There is little apparent difference between heave and the tilt-corrected vertical acceleration under these conditions.

Indeed, in bottom panel of the surface elevation is shown as derived directly from uncorrected heave (red), properly tilt-corrected A_z (black). There is very little appreciable difference between the two records.

Further along in the same record, a rogue wave was observed. In the top panel of Fig. 4, we show the recorded A_z , heave, surge, and sway signal as well as the pitch, and roll signals in the middle panel during the passage of the rogue wave. The pitch reaches nearly 25° and the roll goes just below -12° . The resulting tilt-corrected A_z shows a significant departure from the raw heave signal (top panel Fig. 4).

This difference manifests more impressively in the surface elevation. In the bottom panel of Fig. 4, we again show the sea surface elevation with and without tilt correction in black and red, respectively.

The correctly calculated surface elevation signal shows a crest height of ~ 8 m, and the uncorrected surface elevation gives a crest height of ~ 5 m. The crest heights are unambiguously altered. Notice though that for the crest height of the

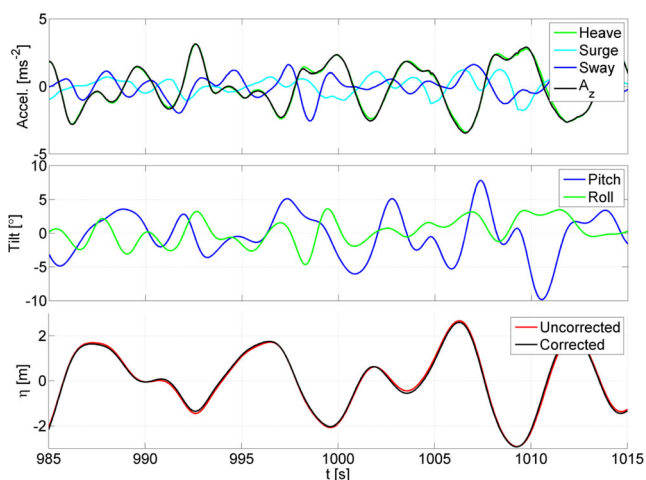


Fig. 3 30-s time series of motion signals and the resulting corrected and uncorrected sea surface elevation. Top panel shows acceleration signals heave (green), surge (cyan), sway (blue), and A_z (black). Middle panel shows rotation signals roll (green), pitch (blue). Bottom panel shows the sea surface elevation calculated directly from heave (uncorrected) in red and the same calculated from the tilt corrected true vertical acceleration, A_z , (corrected) in black

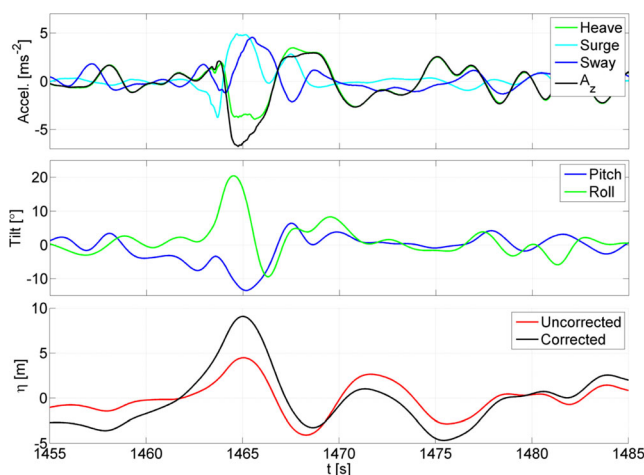


Fig. 4 Thirty seconds of the constituent signals roll (green), pitch (blue), and heave (green) and the resultant true vertical acceleration, A_z (black)

following wave, the trend is the opposite. The corrected wave height is reduced. Clearly, if buoy data are not properly tilt corrected, wave height and crest statistics will be effected, and rogue waves will not be accurately represented.

Figure 5a shows the exceedance distribution functions (EDF) with and without tilt correction. Data were combined from EASI-N and EASI-S. The tilt-corrected data (solid black line) include 3,338,006 apparent waves, and the uncorrected data (solid red line) contain 3,314,960 apparent waves. Following Tayfun and Fedele (2007), theoretical linear EDFs of H take on the general form $P\{H/H_{m0} > AI\} = c_0 f(-AI) \exp(-c_1 AI^2)$, where parameters c_0 and c_1 take on different values and function f takes on different forms to define specific EDFs. In Fig. 5 (all panels), we plot the theoretical EDFs of Rayleigh (linear, Gaussian waves, narrow band assumption), Naess (1985), Boccotti (1989), and Tayfun (1990) using the form and constants from Table 1 in Tayfun and Fedele (2007). The values of c_1 apply to $P\{H/m_0^{1/2} > AI\}$, where m_0 is the first spectral moment (see Eq. 2). Here, c_1 was modified to be applied to $P\{H/H_{m0} > AI\}$. At the scale of Fig. 5a, the EDFs of Naess (blue solid line), Boccotti (cyan solid line), and Tayfun (green solid line) are nearly indistinguishable. They are stratified with EDF of Tayfun on top followed by Boccotti and then Naess. In the range of H/H_{m0} from 0 to 0.5, the field data follow the EDFs of Rayleigh and Tayfun. In the range of H/H_{m0} from 0.5 to 1, field data follow transition to following the EDFs of Boccotti. The field data continue to follow the EDF of Boccotti very closely in range of H/H_{m0} from 1 to 2.

The data in Fig. 5b span the H/H_{m0} values from 1.75 to 2 (rogue criteria). The data are stratified with the tilt-corrected data (solid black line) slightly closer to the Rayleigh EDF (dashed line) followed by the data with no tilt correction (solid red line). The data transition to a departure from the Boccotti EDF towards the Tayfun EDF. Although the effect is not strong in this data, we speculated that ignoring tilt correction, along with reasons described in Forristall (2000), contributed

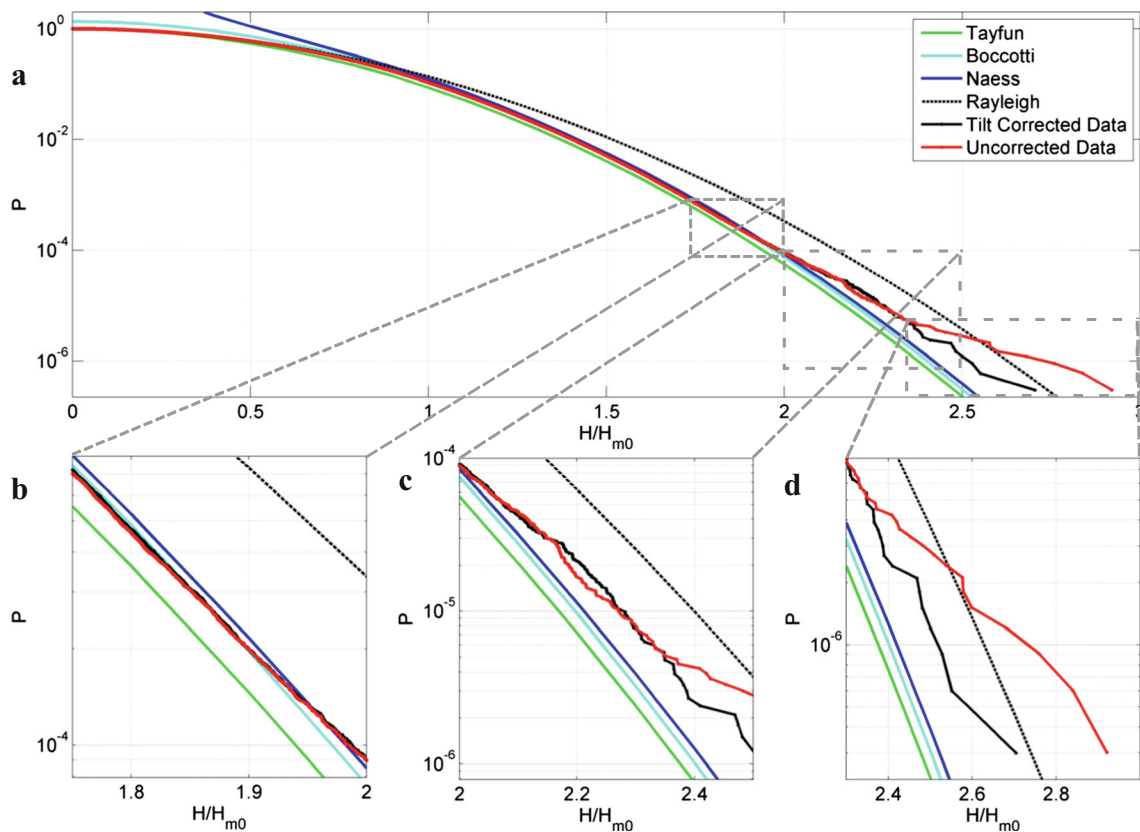


Fig. 5 a Exceedance probability of H/H_{m0} from field data (EASI-N). Solid black line indicates properly tilt-corrected data and solid red line indicates data which have not been tilt corrected. The theoretical EDFs of

Naess (blue solid line), Boccotti (cyan solid line), Tayfun (green solid line), and Rayleigh (black dashed line) are also shown. The panels **b**, **c**, and **d** are zoomed-in subsets of **a**

to past reports of buoy data which give wave crest data which lie far below from that given from a Gaussian (Rayleigh) distribution in the range of $H/H_{m0} < 2$.

In Fig. 5c, which spans H/H_{m0} values from 2 to 2.5, the data lose the stratification and make a departure from EDF of Tayfun. In Fig. 5d, the data span H/H_{m0} values from 2.3 to 2.9. While the corrected data maintain statistics just under the Rayleigh distribution, the uncorrected veer above the Rayleigh distribution.

Bender et al. (2010) dealt with sustained heel (i.e., average leaning or tipping) of a buoy. We have shown that using all degrees of freedom, i.e., all the signals in the motion pack (heave, surge, sway, pitch, roll, yaw) to instantaneously calculate the true vertical acceleration is also important in the time series, not just the mean wave height, even when there is no sustained heel. Depending on details of the buoy rotation and acceleration, not accounting for tilt could spuriously increase or decrease individual wave heights (e.g., bottom panel of Fig. 4). Figure 5 shows that not accounting for tilt results in statistics which depart from the Rayleigh distribution in the range of $H/H_{m0} > 2$. The conclusion is that not tilt correcting may give unrealistic statistics, even in the absence of sustained heel.

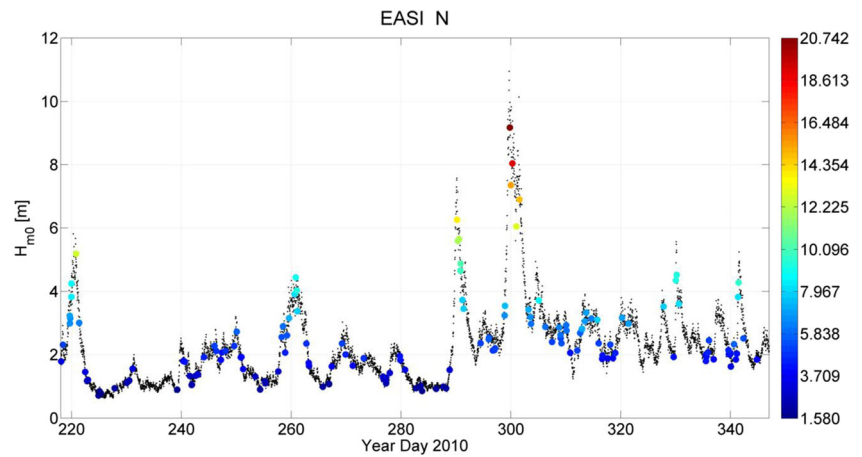
4 Results

For this section, we use the typical rogue wave definition cited above: a single apparent wave, H , (defined by zero-crossing analysis) the height (vertical distance from trough to crest) of which is at least double the significant wave height. Significant wave height may be defined statistically through observed wave height distribution as the mean of the one-third highest wave heights, $H_{1/3}$, or as an integral measure of the 1-D wave spectrum:

$$H_{m0} = 4\sqrt{m_0} = 4\sqrt{\int_0^\infty S(f)df} \tag{2}$$

In the ITOP dataset, $H_{1/3}$ tended to be about 5 % lower than H_{m0} which is consistent with previous studies (Dysthe et al. 2008; Forristall 2000). On the average, H_{m0} is a slightly more selective definition. Since most agencies actually report H_{m0} , not $H_{1/3}$, we choose H_{m0} to define a rogue wave. The ITOP data also showed that down-crossing analysis returned a slightly larger number of total rogue waves compared to up-crossing (158:140, respectively for EASI-N). Quite the

Fig. 6 Time series of H_{m0} as measured by EASI-N (black dots). When an individual wave meets the rogue criterion, a colored dot (the color scale representing the height of the individual wave in meters) is plotted



opposite was found in Pinho et al. (2004), where the number of rogues defined by down-crossing was greatly outnumbered by those defined by up-crossing (108:197, respectively for a Datawell directional waverider). Results shown here are those from down-crossing analysis.

Figure 5a includes 1,837,128 waves measured by EASI-N and 1,500,878 waves measured by EASI-S which makes for a combined 3,338,006 total waves (black line). The combined data from the buoys follow the EDF of Boccotti closely until about the point where $H/H_{m0}=2$. At this point, the data begin to depart from the Boccotti and Tayfun EDFs and approach the Rayleigh distribution. Reiterating the introduction, the measured statistics here are consistent with previous buoy measurements (Dysthe et al. 2008).

Figures 6 and 7 present H_{m0} and H_{max} for the occurrence of the rogue waves. These figures obscure a few rogue waves that occur during the same 30-min block (six and ten in EASI-N and EASI-S, respectively) which are included in the analysis.

These “double rogue” records would be missed by buoys which only record H_{max} and H_{m0} : an advantage of recording the full time series. Rogue waves occurred throughout the ITOP experiment: both in times of relative calm ($H_{m0}<1$ m,

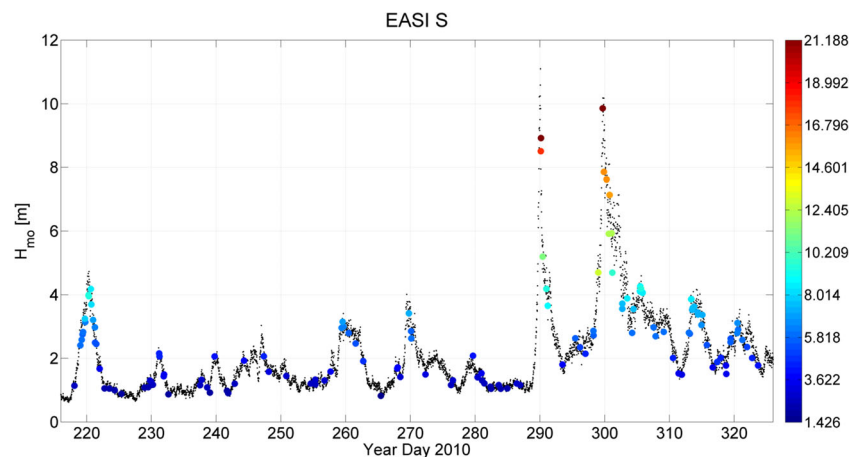
e.g., around year day (YD) 225) and periods of strong forcing ($H_{m0}>8$ m) from Typhoon Chaba around YD 300.

Between EASI-N and EASI-S, a total of 305 waves were recorded which met the rogue criteria, and nine of these had individual wave heights greater than 15 m. The highest individual wave heights recorded for EASI-N and EASI-S were 20.7 and 21.2 m, respectively. Both of these waves met the rogue criteria, for the wave at EASI-N AI=2.26 and at EASI-S AI=2.38. These two waves are shown, along with the full 30-min time series, in Fig. 8. The highest abnormality index recorded was 2.7 ($H_{m0}=5$ m) and was recorded by EASI-S just before YD 300 as Typhoon Chaba was approaching.

4.1 Suggestions for routine measurements

Collins et al. (2014) showed that one may derive directional information from a buoy with a NOMAD-type hull by utilizing all of the motion signals. Utilizing these same signals, one may also tilt correct the heave signal whereby producing true vertical acceleration. Double integrating the vertical acceleration will give an estimation of η and consequently H_{max} . There are still issues with the double integration of acceleration signals which turn up in the record of η as marginal errors.

Fig. 7 Time series of H_{m0} as measured by EASI-S (black dots). When an individual wave meets the rogue criterion, a colored dot (the color scale representing the height of the individual wave in meters) is plotted



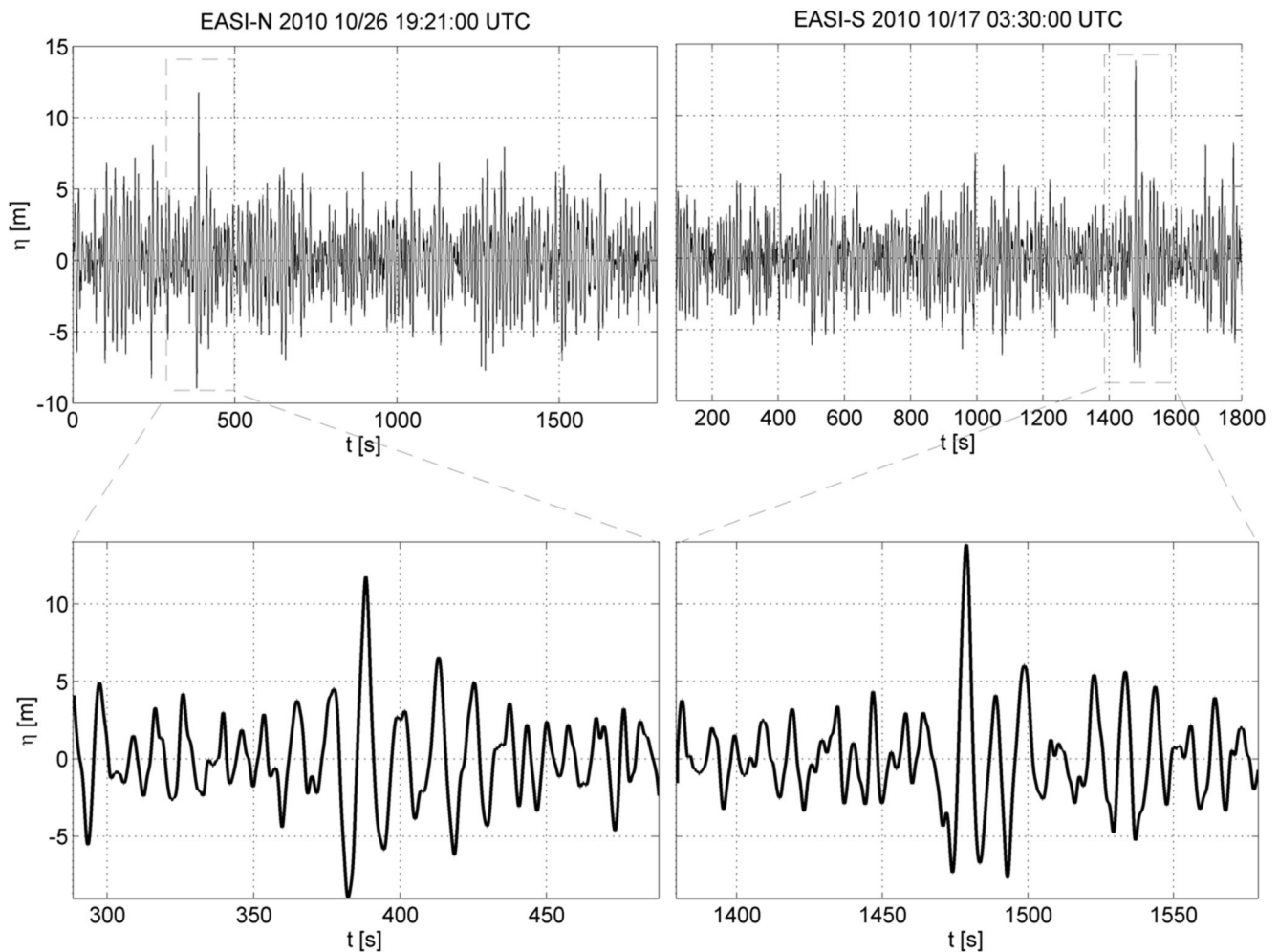


Fig. 8 Largest wave measured by EASI-N and EASI-S on the *left* and *right*, respectively. The *top panels* show the waves in the context of the 30-min run, the *bottom panels* are zoomed-in to show the detailed shape of the waves

Clearly, it would be optimal to keep a full record of η , but this is not done routinely in practice because of data memory limitations. Given this, we offer some suggestions for practices which could be applied to routine measurements of H_{\max} .

- Buoys which do not report direction should be outfitted with motion packages
 - This will increase the stations which are able to report wave direction (Collins III et al. 2014)
 - In addition, the motion package will provide the necessary signals for tilt correction (buoys already reporting direction should possess the necessary signals)
- Acceleration signals must be tilt corrected to give consistent statistics and preserve the shape and height of rogue waves
- In addition to the usual wave parameters, all buoys should report the total number of waves per record (from both zero up- and down-crossing) and H_{\max}

- This would allow for the calculation of AI for every record. If AI is greater than some threshold value (e.g., 2.2) the entire record of η should be saved for further examination
- The margins (the first and last 10 % of the record) should be examined for errors, and H_{\max} which occurs within this range should be suspect

The AI threshold should balance the need to record additional data and concerns of increasing the existing memory load. If these guidelines are adopted, the hope is that there will be an appreciable increase in the records of rogue waves. Such a database should considerably advance our understanding of rogue wave events.

5 Conclusions and future work

The present study introduces a comprehensive, quality controlled, deep-water dataset from the recent ITOP field

experiment, which may offer new insights into rogue waves. We explain in detail the procedures for producing a consistent record of η from an accelerometer buoy. The main result is data which is not tilt corrected, even in the absence of sustained heel, will give unrealistic statistics. In addition, the size and shape of rogue waves may be severely altered without the tilt correction. The corrected data followed closely the theoretical EDF of Boccotti in the range of H/H_{m0} 1–2 and approach the Rayleigh EDF outside of this range.

Though the potential for future efforts using this dataset is great, it is hoped that the lessons learned here might be applied to routine measurements made by various government agencies. Some suggested guidelines were offered for making these measurements. It is believed that, should recording rogue waves be made routine, a dataset of unprecedented potential will be produced. This dataset would serve our understanding of the nature of rogue waves. It is hoped that later findings will make sea travel and operations safer.

Here, analysis was focused on the time domain, but, there is interest in understanding the spatial distribution of wave parameters in tropical cyclones and what this implies for the probability and occurrence of rogue waves (Mori 2012). It is planned to further analyze the data to see if spectral parameters dependent on quadrant and distance from radius of maximum winds (RMW) in way consistent with previous studies. It needs to be noted that this dataset, although relatively rich and unique, is hardly exhaustive in terms of quadrant sampling, storm strength, RMW, storm translation speed, directional change of the storm translation, and other storm parameters. If measurements of H_{\max} were made routinely available, then, a thorough study of this type will be possible using composite measurements from many buoys and many storms (e.g., the method employed by Hu and Chen (2011)).

Acknowledgments COCIII would like to acknowledge friends at the University of Tokyo who were very generous and hospitable during the summer of 2013. Thanks to RSMAS professors Dr. C. Linwood Vincent, Dr. William M. Drennan, and Dr. Brian K. Haus for useful conversation regarding this and other related work. The insightful comments of two anonymous reviewers were very much appreciated. Ms. Erin Middleton helped revise an early draft. Thanks to the captains and crew of the R/V Roger Revelle. ITOP funding was provided by the U.S. Office of Naval Research grant #N00014-09-0392. Part of this work was done at the University of Tokyo under a National Science Foundation EAPSI fellowship which is a joint partnership with the Japanese Society for the Promotion of Science summer program.

References

- Antcl F, Donelan MA, Drennan WM (1994) Eddy-correlation measurements of air-sea fluxes from a discus buoy. *J Atmos Ocean Technol* 11:1144–1150
- Bender LCI, Guinasso NLJ, Walpert JN, Howden SD (2010) A comparison of methods for determining significant wave heights-applied to a 3 m discus buoy during Hurricane Katrina. *J Atmos Ocean Technol* 27:1012–1028
- Boccotti P (1989) On mechanics of irregular gravity waves. *Atti Accad Nazionale Dei Lincei, Mem VIII* 19:111–170
- Cavaleri, L., Bertotti, L., Torrisi, L., Bitner-Gregersen, E., Serio, M., & Onorato, M. (2012). Rogue waves in crossing seas: The Louis Majesty accident. *J Geophys Res: Oceans* (1978–2012), 117(C11)
- Chuang, L., Wu, L., Lin, C., & Kao, C. C. (2009). Applying the wavelet transform to derive sea surface elevation from acceleration signals. *OCEANS 2009, MTS/IEEE Biloxi-Mar Technol Futur: Glob Local Chall*, pp. 1-5
- Collins III, C.O., B. Lund, R.J. Ramos, W.M. Drennan, H.C. Graber (2014). Wave measurement intercomparison and platform evaluation during the ITOP (2010) experiment. (Submitted for publication)
- D’Asaro, E. A., Black, P. G., Centurioni, L., Chang, Y., Chen, S. S., Foster, R., et al. (2013). Impact of typhoons on the ocean in the pacific: ITOP. *Bull Am Meteorol Soc*
- Doong, D., & Wu, L. (2010). Searching for freak waves from in-situ buoy measurements. *OCEANS 2010 IEEE-Sydney*, pp. 1-6
- Drennan, W.M., H.C. Graber, C.O. Collins III, A. Herrera, H. Potter, R.J. Ramos, N.J. Williams (2014) EASI: An air-sea interaction buoy for high winds. *J Atmos Ocean Technol*. doi:10.1175/JTECH-D-13-00201.1
- Dysthe K, Krogstad HE, Müller P (2008) Oceanic rogue waves. *Annu Rev Fluid Mech* 40(1):287–310
- Forristall GZ (2000) Wave crest distributions: observations and second-order theory. *J Phys Oceanogr* 30(8):1931–1943
- Forristall GZ, Barstow SF, Krogstad HE, Prevosto M, Taylor PH, Tromans P (2002) Wave crest sensor intercomparison study: an overview of WACSIS. 21st International Conference on Offshore Mechanics and Arctic Engineering, Oslo
- Graber HC, Terray EA, Donelan MA, Drennan WM, van Leer JC, Peters DB (2000) ASIS—a new air–sea interaction spar buoy: design and performance at sea. *J Atmos Ocean Technol* 17(5): 708–720
- Guedes Soares C, Cherneva Z, Antão EM (2004) Abnormal waves during Hurricane Camille. *J Geophys Res* 109, C08008
- Hu K, Chen Q (2011) Directional spectra of hurricane-generated waves in the Gulf of Mexico. *Geophys Res Lett* 38(19), L19608
- Krogstad HE, Barstow SF (2000) Unified approach to extreme value analysis of ocean waves. *Proc Int Offshore Polar Eng Conf* 3:103–108
- Magnusson AK, Donelan MA (2013) The Andrea wave characteristics of a measured North Sea rogue wave. *J Offshore Mech Arctic Eng* 135(3)
- Mori N (2012) Freak waves under typhoon conditions. *J Geophys Res* 117:C00J07
- Naess A (1985) On the distribution of crest to trough wave heights. *Ocean Eng* 12(3):221–234
- Onorato M, Waseda T, Toffoli A, Cavaleri L, Gramstad O, Janssen PAEM et al (2009) Statistical properties of directional ocean waves: the role of the modulational instability in the formation of extreme events. *Phys Rev Lett* 102(11):114502
- Pinho U, Liu PC, Ribeira C (2004) Freak waves at Campos basin, Brazil. *Geofizika* 21:53–66
- Srokosz MA, Longuet-Higgins MS (1986) On the skewness of sea-surface elevation. *J Fluid Mech* 164:487
- Steele KE, Lau JC, Hsu YL (1985) Theory and application of calibration techniques for an NDBC directional wave measurements buoy. *IEEE J Ocean Eng* 10(4):382–396
- Tamura H, Waseda T, Miyazawa Y (2009) Freakish sea state and swell-windsea coupling: Numerical study of the Suwa-Maruru incident. *Geophys Res Lett* 36(1), L01607

- Tayfun MA (1990) Distribution of large wave heights. *J Waterw Port Coast Ocean Eng* 116(6):686–707
- Tayfun MA, Fedele F (2007) Wave-height distributions and nonlinear effects. *Ocean Eng* 34(11):1631–1649
- Waseda T, Kinoshita T, Tamura H (2009) Evolution of a random directional wave and freak wave occurrence. *J Phys Oceanogr* 39(3): 621–631, 634–639
- Waseda T, Hallerstig M, Ozaki K, Tomita H (2011) Enhanced freak wave occurrence with narrow directional spectrum in the North Sea. *Geophys Res Lett* 38(13)
- Waseda T, Tamura H, Kinoshita T (2012) Freakish sea index and sea states during ship accidents. *J Mar Sci Technol* 17(3):305–314
- Young I (1994) On the measurement of directional wave spectra. *Appl Ocean Res* 16(5):283–294